Supporting Information

Salt-responsive evaporation behavior of chitosan-based hydrogels: driven by dual-mechanism synergy for efficient seawater desalination

*Cheng-Shuai Shu[1], Lin-Hui Zhang[1], Jun-Yi Zhang[1], Xiao-Rong Sun[1], Chang-Ping Feng[2], Lu Bai[1], Jie Yang[1,] *, Wei Yang[1,] **

[1]College of Polymer Science and Engineering, Sichuan University, State Key Laboratory of Advanced Polymer Materials, Chengdu 610065, Sichuan, P. R. China

[2]Shandong Engineering Research Center for Additive Manufacturing, Qingdao University of Technology, Qingdao 266520, Shandong, P. R. China

*Corresponding authors: psejieyang@scu.edu.cn (J. Yang); weiyang@scu.edu.cn (W. Yang)

Section S1.1 Estimation of the equivalent vaporization enthalpy

The equivalent vaporization enthalpy (E_{equ}) is calculated based on the assumption that the energy input from the environment is identical for both the bulk water and the hydrogel under dark conditions. The device was enclosed in a sealed environment with a stabilized humidity of *ca*. 45% and a temperature of *ca*. 25 °C. Accordingly, E_{equ} of the hydrogel in this system can be estimated by its evaporation rate, which is expressed by equation (S1):

$$E_{equ} = \frac{E_0 m_0}{m_1} \#(S1)$$

where E_0 is the evaporation enthalpy of pure water obtained by DSC measurements (Fig. 3g, 2413 J g^{-1}), and m_0 and m_1 are the mass changes of bulk water and the hydrogel, respectively.

Section S1.2 Calculation of Solar-to-vapor Conversion Efficiency and Energy Balance Analysis

The apparent solar-to-vapor conversion efficiency (η_a) refers to the percentage of solar energy utilized for effective water evaporation, which can be calculated by equation (S2):

$$\eta_a = \frac{vE_{equ}}{C_{opt} p_n} \#(S2)$$

where v is the steady-state evaporation rate, $E_{equ}$is the equivalent evaporation enthalpy of hydrogels obtained by dark evaporation experiments (Fig. 3i), C_{opt} is the optical concentration, and p_n is the normal illumination intensity of one sun (1 kW m^{-2}). The calculated solar-to-vapor conversion efficiencies of CCH1-DF and CH1-DF were 95.74% and 24.05%, respectively.

To further validate the reliability of the high apparent solar-to-vapor conversion efficiency, a detailed energy balance analysis was conducted, which includes the net solar-driven evaporation efficiency (η_{net}) and various non-evaporative heat losses. The

η_{net} refers to the energy utilization efficiency contributed solely by solar irradiation, obtained by subtracting the contribution of dark evaporation from the total evaporation rate, which can be calculated by equation (S3):

$$\eta_{net} = \frac{(v - v_{dark})E_{equ}}{C_{opt}p_n} \#(S3)$$

where v_{dark} is the dark evaporation rate (0.38 kg m^{-2} h^{-1}) obtained from the dark evaporation test. The η_{net} calculated through this equation is 79.91%.

The non-evaporative heat losses, including radiation (η_{rad}), convection (η_{conv}), and conduction (η_{cond}), can be calculated by equations (S4-6):

$$\eta_{rad} = \epsilon\sigma(T_s^4 - T_a^4) \#(S4)$$

$$\eta_{conv} = h(T_s - T_a) \#(S5)$$

$$\eta_{cond} = \frac{C_p m \Delta T}{At} \#(S6)$$

where ϵ is the emissivity (0.95), σ is the Stefan-Boltzmann constant, T_s is the steady-state surface temperature, T_a is the ambient temperature, h is the convective heat transfer coefficient (5 W m^{-2} k^{-1}), C_p is the specific heat capacity of water (4.2 J g^{-1} $°C^{-1}$), m is the total mass of the bulk water, ΔT is the temperature rise in bulk water, A is the illuminated area at the top of the evaporator, and t is the duration under illumination. According to the calculation, the η_{rad}, η_{conv}, and η_{cond} of the CCH1-DF evaporator is 15.31%, 11.75% and 3.27%, respectively.

The intrinsic solar-to-vapor conversion efficiency (η_i) is defined and can be calculated by equation (S7):

$$\eta_i = \eta_{net} + \eta_{rad} + \eta_{conv} + \eta_{cond} \#(S7)$$

Based on the calculations, the intrinsic solar-to-vapor conversion efficiency is 110.24%. This phenomenon, where the value apparently exceeds 100%, arises because the energy input is calculated solely based on the two-dimensional illuminated area at the top of the evaporator. In realistic conditions, and the thickness of the evaporator

provides additional side surface area that serves as a supplementary pathway for vapor escape, thereby increasing the actual evaporation area and reducing the diffusion resistance. Furthermore, the top illuminated area of the evaporator is not perfectly smooth, which leads to an enlargement of the actual light-absorbing area. Both the three-dimensional edge effect and the surface micro-roughness synergistically contribute to the observed enhancement in apparent efficiency.

Supplementary figures and tables

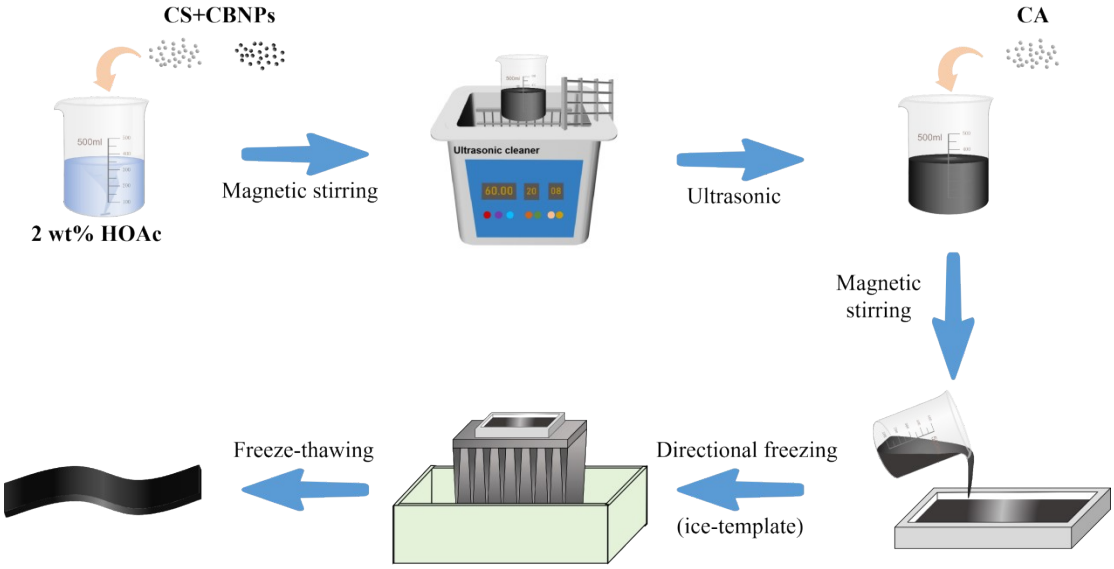

Fig. S1 Schematic of the preparation process of CCHx-NF hydrogel.

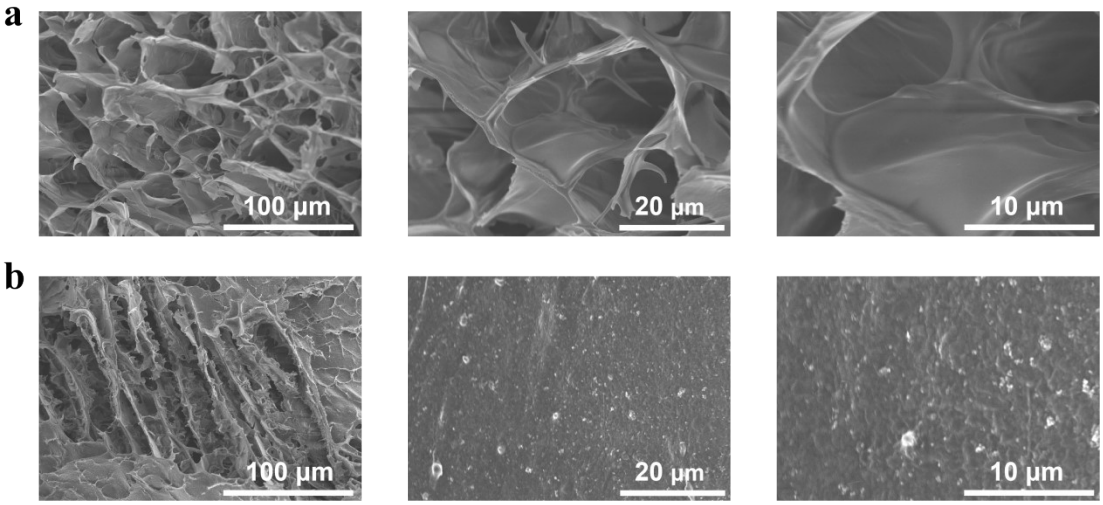

Fig. S2 Cross-sectional SEM images of the (a) CH1-DF hydrogel and (b) CCH1-DF hydrogel.

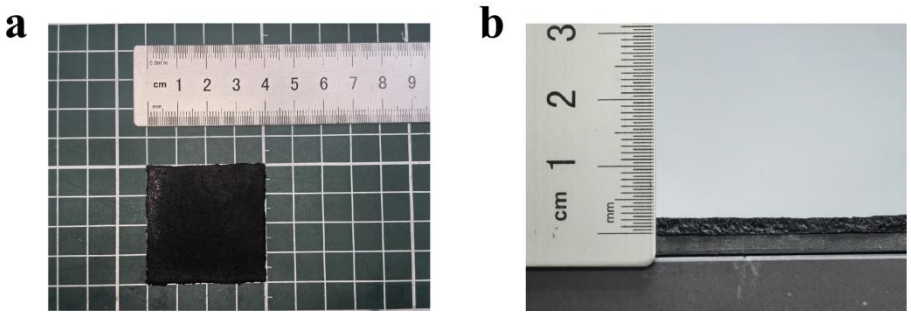

Fig. S3 Optical photographs showing the (a) top and (b) side views of the CCH1-DF hydrogel.

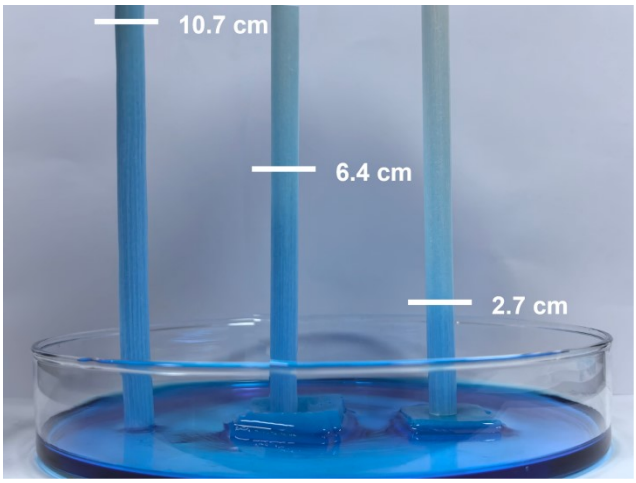

Fig. S4 Water transport assessment using commercial cotton wicks placed on the surfaces of CCH1-DF and CCH1-NF.

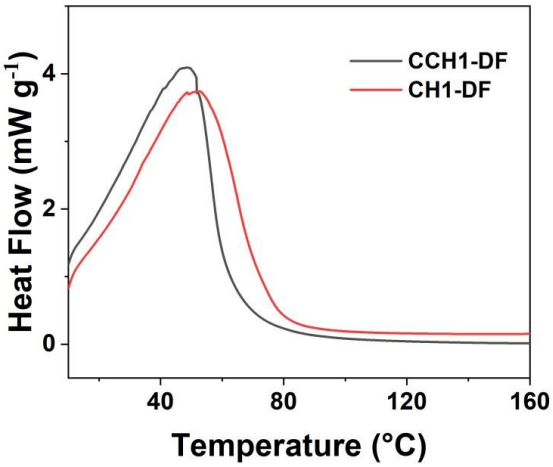

Fig. S5 DSC heat flow curves of the swollen CCH1-DF and CH1-DF hydrogels.

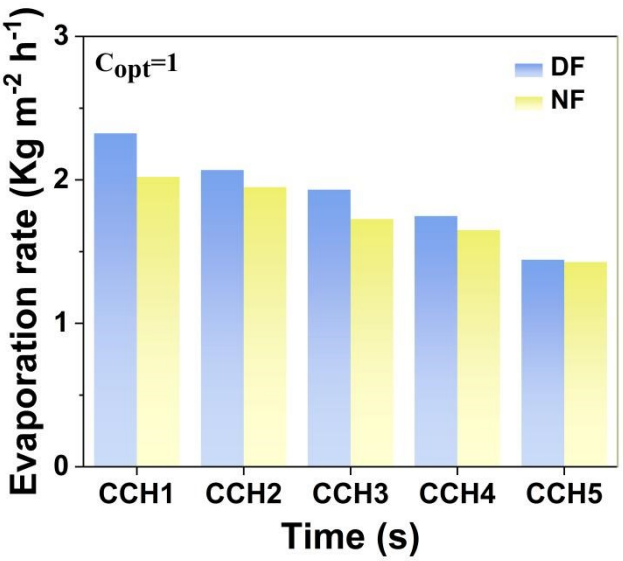

Fig. S6 Simulated solar evaporation performance of CCHx-DF and CCHx-NF.

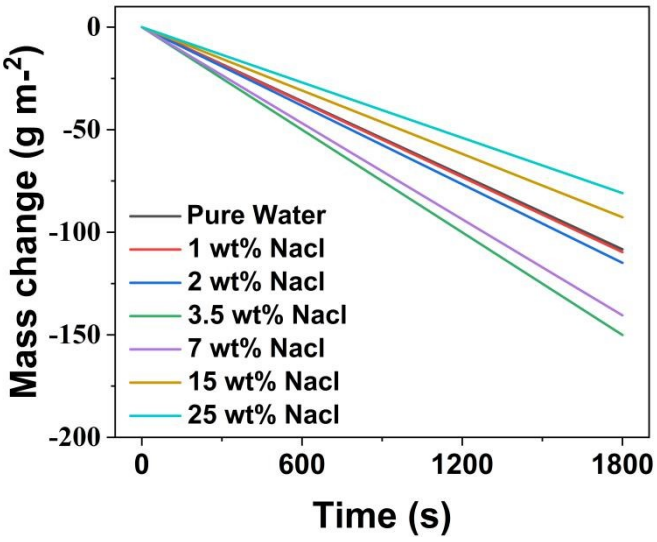

Fig. S7 Dark evaporation rates of CCH1-DF hydrogel in NaCl solutions with various concentrations.

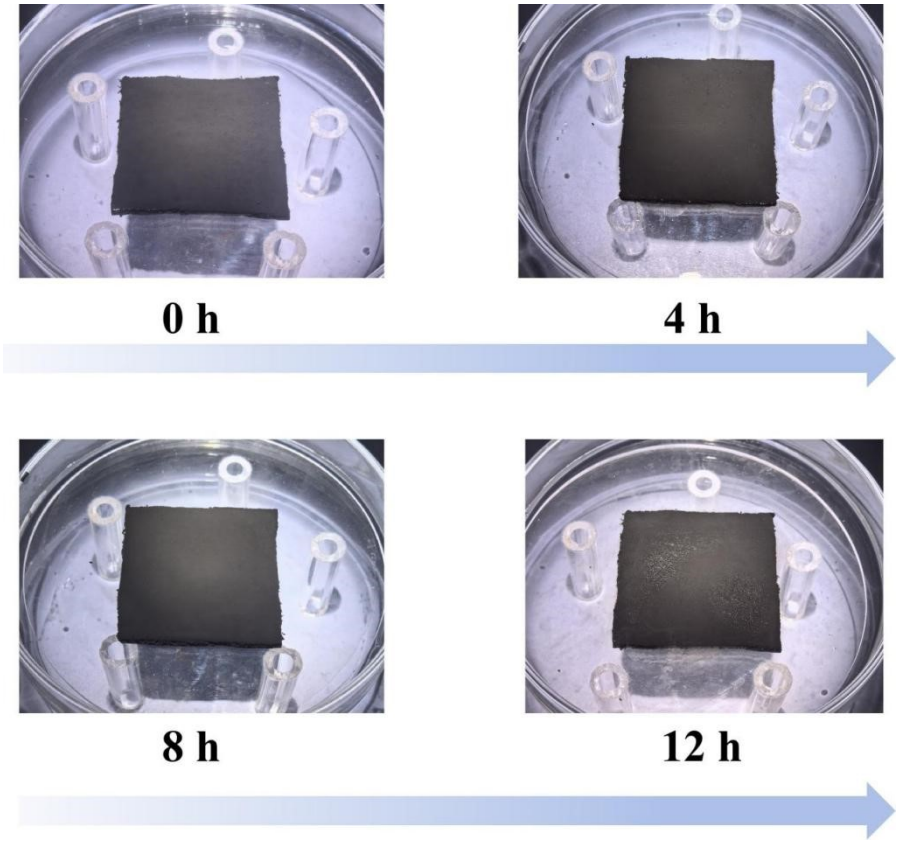

Fig. S8 Salt tolerance of the CCH1-DF hydrogel. Digital photographs of the CCH1-DF evaporator surface after continuous simulated solar evaporation for 12 hours in 15 wt% NaCl solution.

Evaporator	Evaporation rate (kg m^{-2} h^{-1})	Evaporation efficiency (%)	Refs
Lignin hydrogel	2.25	91.88	2022[S1]
Chitosan@carbon nano tubes aerogel	1.54	91.47	2024[S2]
PVA@tobacco leaves hydrogel	1.07	74.3	2024[S3]
Chitosan/MXene aerogel	1.68	75	2024[S4]
Chitosan-lignosulfonate sodium hybrid hydrogel	2.37	-	2024[S5]
Sodium alginate hydrogel	2.42	96.7	2025[S6]
Cellulose nanofiber - lignosulfonate hydrogel	1.75	-	2025[S7]
Phytic acid-PVA-chitosan hydrogel	2.52	-	2026[S8]
PVA hydrogel enhanced biomass loofah	1.82	94.81	2026[S9]
CCH1-DF	**2.98**	**95.82**	**This work**

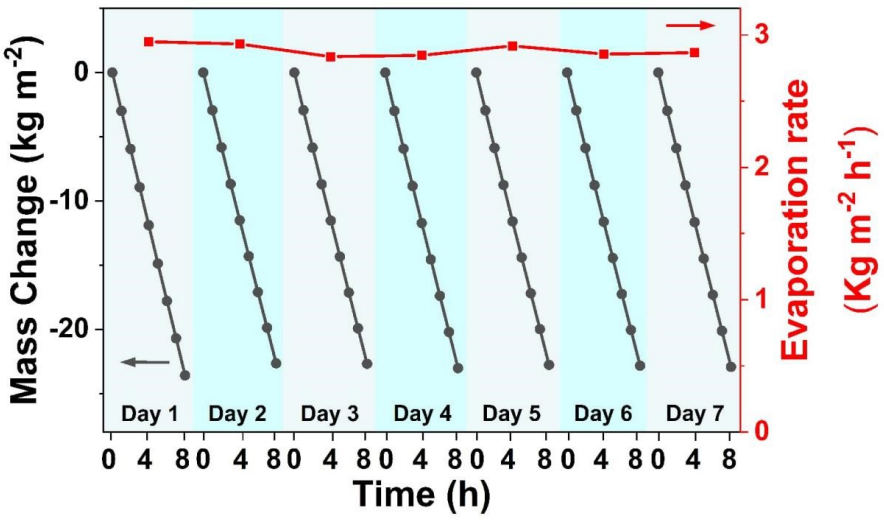

Fig. S9 Mass change curves and the corresponding evaporation rate of CCH1-DF during the 7-day cycling experiment, with 8 hours of exposure to 1 kW m^{-2} solar irradiation every day.

Table S1. Comparison of the solar vapor generation performance and evaporation efficiency of the proposed CCH1-DF evaporator with other previously reported evaporators in a 3.5 wt% NaCl solution.

References

S1 S. Jiang, Z. Zhang, T. Zhou, S. Duan, Z. Yang, Y. Ju, C. Jia, X. Lu and F. Chen, *Desalination*, 2022, **531**, 115706.

S2 Y. Xue, X. Han, D. Xu, Z. Zhang, L. Zhu and S. Wang, *Desalination*, 2024, **575**, 117333.

S3 Z. Wang, L. Han, G. Xi, T. Jia, Y. Liu, X. He, H. Wang and B. Li, *RSC Sustain.*, 2024, **2**, 1081-1087.

S4 F. Zhang, Z. Qi, X. Han, H. Cai and K. Yang, *Sustain. Energy Fuels*, 2024, **8**, 3680-3687.

S5 P. Wang, X. Wang, X. Wang, X. Lin and X. Qiu, *Chem Bio Eng.*, 2024, **1**, 252-263.

S6 N. An, M. Ma, Y. Chen, Z. Wang and Q. Li, *ACS EST Eng.*, 2025, **5**, 732-742.

S7 J. Zhu, C. Shao, S. Hao, J. Zhang, W. Ren, B. Wang, L. Xiao, H. Lei, T. X. Liu, Z. Yuan and R. Sun, *Adv. Sci.*, 2025, **12**, e13258.

S8 L. Hao, R. Zhang, Y. Xu, J. Lu, H. Zhang, X. Kong, Y. Xiang, G. Yang and Y. Chang, *ACS Appl. Mater. Interfaces*, 2026, **18**, 8783-8795.

S9 L. Rao, Y. Liu, S. Zhu, G. Zhong, M. Wen, K. Xu, S. Yu, S. Wang and X. Niu, *Renew. Energy*, 2026, **256**, 123958.